

CRUSTAL MOVEMENT DETECTION FOR THE 2011 TOHOKU, JAPAN EARTHQUAKE FROM MULTI-TEMPORAL TERRASAR-X INTENSITY IMAGES

Wen Liu¹⁾ and Fumio Yamazaki²⁾

1) *PhD student, Dept. of Urban Environment Systems, Chiba University, Japan; JSPS research fellow*

2) *Professor, Dept. of Urban Environment Systems, Chiba University, Japan*

Wen_liu@graduate.chiba-u.jp, fumio.yamazaki@faculty.chiba-u.jp

Abstract: About 5.3 m crustal movement in the horizontal direction and 1.2 m in the vertical direction were observed by GPS ground station in the Tohoku earthquake, which occurred on March 11, 2011. In this study, a pre-event TerraSAR-X image of Tohoku area, taken on Oct. 21, 2010 and three post-event images taken on March 13, 24 and April 4, 2011 were used to estimate the constant crustal movements by a subpixel level area-based matching method. Firstly, the unchanged buildings were extracted by segmentation using the high backscatter coefficient. Next, the slide distance of an unchanged building was calculated by the area-based matching, using the surrounding area from pre- and post-event images. To enhance the accuracy of measurement, the original images were resized to 0.25m/pixel, as 1/5 of the original pixel size. Finally, the crustal movement in a unit area was obtained by averaging the buildings' movements in this area. The results were compared with the GPS observed data, and the crustal movement was found to be estimated in high accuracy by the proposed method.

1. INTRODUCTION

The M_w 9.0 Tohoku Earthquake on March 11, 2011, which occurred off the Pacific coast of the northeastern (Tohoku) Japan, caused gigantic tsunamis and brought vast devastation, and thus many people were lost their lives. The epicenter was located at 38.322°N, 142.369 °E at a depth of about 32 km. The earthquake was resulted from a thrust faulting on or near the subduction zone plate boundary between the Pacific and North America plates. According to the GPS Earth Observation Network System (GEONET) of the Geospatial Information Authority (GSI) of Japan, crustal movements more than 5 m at the maximum in the horizontal direction and 1 m at the maximum in the vertical direction were observed in a wide area (GSI, 2011). Although GSI has established about 1,200 GPS ground control stations over all of Japan, the distance between two neighboring stations is over 20 km. Hence it is still difficult to grasp detailed crustal movement distribution just from the GPS recording data.

Interferometric analysis of synthetic aperture radar (SAR) is one of the powerful tools to map the ground deformation (Massonnet et al. 1993). Several researches have carried out the approach to detect the displacements due to earthquakes by differential SAR interferometry (DInSAR) (Stramondo et al. 2002; Chini et al. 2010). However, depending on vegetation and temporal decorrelation, InSAR may not be able to measure ubiquitous deformation at a large scale. Also, InSAR can only detect the deformation in the range direction of sensor. A pixel-offset method was proposed to detect the deformation

from SAR and optical images (Michel et al. 1999; Tobita et al. 2006). By this method, two images were co-registered firstly. Then the local deformation was calculated by cross-correlation. However, in the 2011 Tohoku earthquake, the extent of crustal movements was much larger than the image covering area. If the registration is applied to a pair of pre- and post-event satellite images, the crustal movements would be diminished. Hence, the standard pixel-offset method is not suitable to detect the absolute crustal movements in this earthquake.

In this study, four temporal TSX intensity images taken before and after the Tohoku earthquake are used to detect crustal movements from the shifts of unchanged buildings. Then the accuracy of the proposed method is demonstrated by comparing the detected displacements with those from GPS ground station records.

2. IMAGE DATA AND PROCESSING

The study area was focused on the coastal zone of Tohoku, Japan, as shown in Figure 1(a), which was one of the most severely affected areas during the 2011 Tohoku earthquake. Four temporal TSX images taken before and after the earthquake are shown in Figure 1(b-e), which we used for detecting crustal movements. The pre-event image was taken on October 20, 2010 (UTC), while the post-event ones were taken on March 12 (two days after the earthquake) and 23, and April 3, 2011. There is a 37.31° incidence angle at the center of the images. All images were captured with HH polarization and in a descending path.

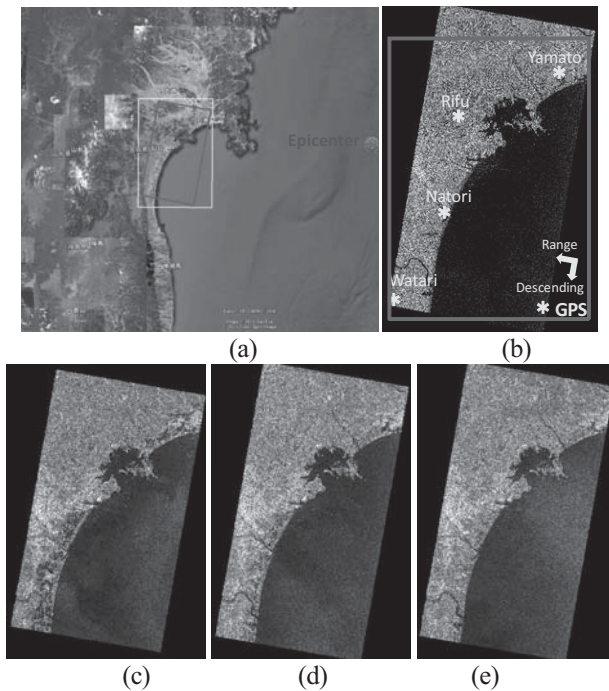


Figure 1 Study area on the Pacific coast of Tohoku, Japan (a) including four GPS ground stations; the pre-event TSX image taken on Oct. 21, 2010 (b); and the post-event images taken on March 13 (c), 24 (d), and April 4 (e), 2011.

Images were acquired in the StripMap mode, so the azimuth resolution was about 3.3 m while the ground range resolution was about 1.2 m. The images were orthorectified multi-look corrected products (EEC), where the image distortion caused by variable terrain height was compensated for by using a globally available DEM (SRTM). Therefore, they have been resampled and projected to a WGS84 reference ellipsoid with a square pixel size of 1.25 m.

Two preprocessing approaches were applied to the images before extracting the crustal movements. First, the four TSX images were transformed to a Sigma Naught (σ^0) value, which represents the radar reflectivity per unit area in the ground range. A Lee filter (Lee 1980) was then applied to the original SAR images to reduce the speckle noise, which makes the radiometric and textural aspects less efficient although it improves the correlation coefficient between the two images. To minimize any loss of information included in the intensity images, the window size of the Lee filter was set as 3×3 pixels (approximately 3.8×3.8 m). Registration is typically necessary during the preprocessing stage. However, the crustal movements of this earthquake occurred in all image areas, so the movement detected would be a relative movement if the pre- and post-event TSX images were registered. Thus, the pixel localization corrected by the GPS orbit determination was used directly in this study. According to the product specification document publicized by DLR, the achieved orbit accuracy error is considered to be below 20 cm (Eineder et al. 2010).

3. METHODOLOGY

This study proposes a method for detecting crustal movements based on the measurement of the movements of unchanged buildings in SAR intensity images. In current methods, crustal movements are usually detected by registering ground surface. However, during the Tohoku earthquake, a gigantic tsunami hit many cities/towns along the coast and the ground surface was changed significantly by debris or flooded seawater. Thus, our study focused on the movements of unchanged buildings to ensure a stable correlation and highly accurate movement detection. First, segmentation was performed on both images to extract the location of building objects. Next, matching was introduced to detect unchanged buildings. The displacements of unchanged buildings were calculated using an area-based matching method. Finally, all the movements of unchanged buildings were obtained, and they were considered to be the crustal movements in the study area.

3.1 Segmentation and extraction

In most cases, buildings show a higher backscatter than other surface objects in SAR images because of their corner reflection. To detect the locations of buildings, we performed segmentation on the pre- and post-event TSX images. According to a visual inspection of the histograms of the SAR images, the threshold value of the backscattering coefficient between buildings and other objects was set as -2.0 dB. Based on a typical building size, only objects larger than 100 pixels (about 150 m^2) were extracted as engineered (solid) buildings. Thus, objects with an average backscattering coefficient greater than -2.0 dB and larger than 100 pixels were extracted and used in the next step. Part of the color composition of the pre- and post-event building images is shown in Figure 2(a). Obvious shifts can be seen in the shapes of the same buildings between images.

The tsunami caused by the earthquake affected vast amounts of coastal areas, so many constructions such as wooden houses and seawalls were destroyed or carried away. Thus, the shifts of unchanged buildings had to be observed to measure the crustal movements. A building object extracted from the pre-event building image was selected as a target object. A rectangular area surrounding the target building and exceeding its size was then selected from the post-event building image as the search area. An example of the target and search areas is shown in Figure 2(b). If a building object existed in this area, then the target building was considered as unchanged. Based on the GPS ground control points data, the maximum crustal movement observed during this earthquake was about 5 m, so the search area was set as 5 pixels (6.25 m) larger than the target object in every direction.

3.2 Calculation

After detecting the locations of unchanged buildings, the shifts of building shapes due to the earthquake were

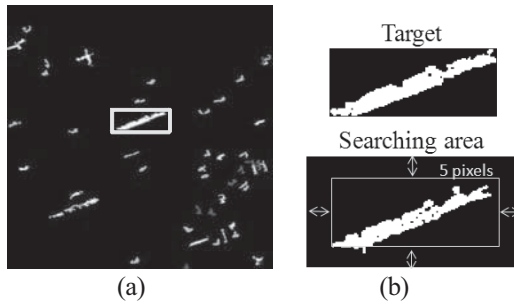


Figure 2 Color composition of pre- and post-event building images (a); a target building object in the pre-event and the search area in the post-event building image (b)

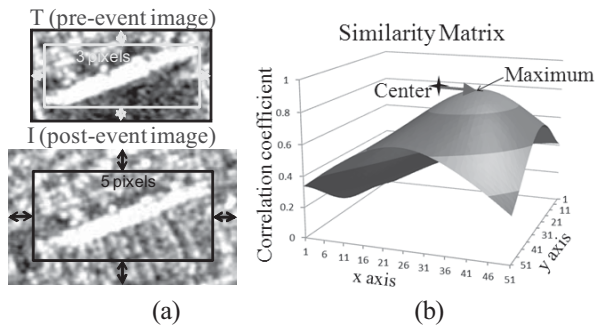


Figure 3 Target area T in the pre-event and the search area I surrounding the target area in the post-event SAR image (a); similarity matrix for the target and search areas (b).

calculated using an area-based method. The target area (T) was selected from the pre-event intensity image in the locations of unchanged building objects, which were extracted in the previous step. To improve the accuracy of area-based matching, the ground surface surrounding the building object within a distance of 3 pixels was also included in the target area. The search area (I) was selected in the post-event intensity image, which surrounded the target area and exceeded it in size. Examples of T and I are shown in Figure 3(a). The target and search areas were resampled to 0.25 m/pixel by cubic convolution to 1/5 of the original pixel size. The shift of building shapes could then be detected at a sub-pixel level.

Area correlation is a method used for designating GCPs during image-to-image registration. In this study, the target area was overlaid with the search area and a similarity index was calculated. The similarity matrix contained the values of the statistical comparison between the target and search areas. The position in the similarity matrix where the similarity index reached a maximum value represented the necessary offset that the target had to move along the x- and y-axes to match the searching area.

An example of a calculated similarity matrix is shown in Figure 3(b). The target and search areas were selected with the same center point, so the maximum value should be at the center of the matrix if no movement occurred. In this case, the building moved 11 pixels to the east and 5 pixels to the south, which indicated that the crustal movement in this area was 2.75 m to the east and 1.25 m to the south.

4. RESULTS

The TSX images in the red frame of Figure 1(a) were divided into a square mesh containing 2000×2000 pixels ($2.5 \times 2.5 \text{ km}^2$), to detect the ground movements. The movements of unchanged buildings were calculated in each sub-area and the average value was considered to be the crustal movement of that sub-area. A square including the GPS ground control station, known as Yamoto, is shown in Figure 4(a). We extracted 107 buildings from the pre-event image, whereas 85 buildings were detected as unchanged between the Oct. 21, 2010 and March 13, 2011 images. These buildings were mostly distributed outside the areas inundated by the tsunami. To ensure that the pre-event building matched with the same post-event building correctly, only the shift of a building with a similarity index higher than 0.8 was counted as a crustal movement. Using this method, the shifts of 67 buildings were detected in this square area and their movement vectors are shown in Figure 4(a), with histograms of the movements in the east and north directions. The mean value of the displacement was 3.66 m, heading toward 107.40° clockwise from the north.

The crustal movements over the whole area were detected in the same way. To ensure the reliability of the results, only a sub-area containing more than 5 building displacements was counted as a valid sub-area. Thus, several sub-areas in mountain region were not valid. The results of the other squares including GPS ground control stations Rifu, and Watari, are shown in Figure 4(b-c). The shifts of 99 buildings were detected in the square of Rifu. The mean value of the displacement was 3.07 m, heading toward 103.71° clockwise from the north. And there were the shifts of 63 buildings detected in the square of Watari. The mean value of the displacement was 2.82 m, heading toward 99.57° clockwise from the north. Since there were few buildings surrounded Natori ground station, the detected shifts in this square were only 3, seen as an invalid mesh. The displacement vectors throughout the image are shown in Figure 5(a) and the distance maps is shown in Figure 6(a). A comparison of the movements detected surrounding GPS stations shows that the largest movement occurred around Yamoto station and it was smaller when moving southwards. The angular heading of the detected movements moved nearer to the east when heading southwards. The same trend was observed in the displacement vectors over all the studied area. This trend matched the observed GPS data. Based on the standard deviation of the movements in the east and north directions, we can see that most motion vectors pointed to the same direction in each sub-area. However, several arrows still pointed in different directions, which were errors. These errors occurred during the matching step. In this earthquake, the crustal movements were very large, with more than 5 m horizontal shifts in some areas. Thus, the search area was sufficiently large to include similar neighboring buildings, which led to mismatching.

Crustal movements were also detected in the periods Oct. 21, 2010 to March 24, 2011, and Oct. 21, 2010 to April

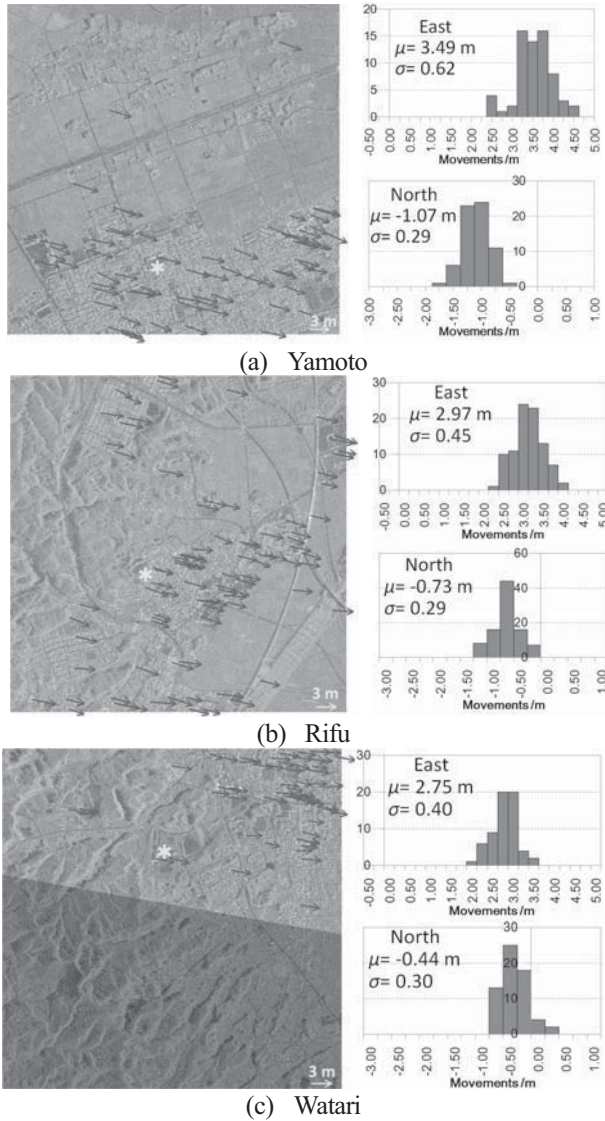


Figure 4 Results showing the displacement vectors detected between Oct. 21, 2010 and March 13, 2011 images, which overlap on the color composite of the TSX intensity images, with the mesh including Yamoto (a), Rifu (b) and Watari (c) GPS station, and histograms showing the displacements to the east and north directions.

4, 2011. Their displacement vectors are also shown in Figure 5(b-c) and the distance maps are shown in Figure 6(b-c). We compared the results over three different periods and the movements detected were larger as time passed, which also agreed with the GPS data. Large movements can be seen in northern areas close the coast. An averaged displacement of about 0.32 m occurred between March 13 and 24, while an averaged movement of about 0.06 m occurred between March 24 and April 4. Based on these results, we have shown that our method is also useful for measuring gradual movements after a main shock.

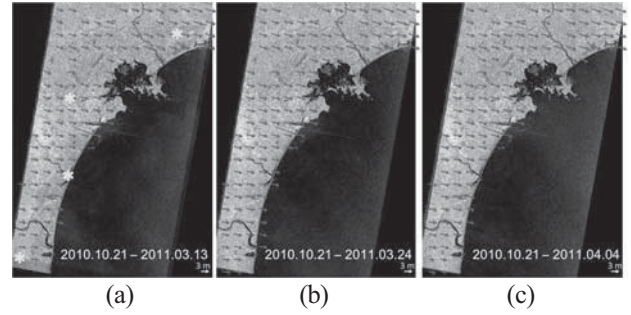


Figure 5 Detected displacement vectors in each sub-area in the periods: Oct. 21, 2010 to March 13 (a), to March 24 (b) and to April 4, 2011 (c), overlapping on the color composite of the TSX intensity images.

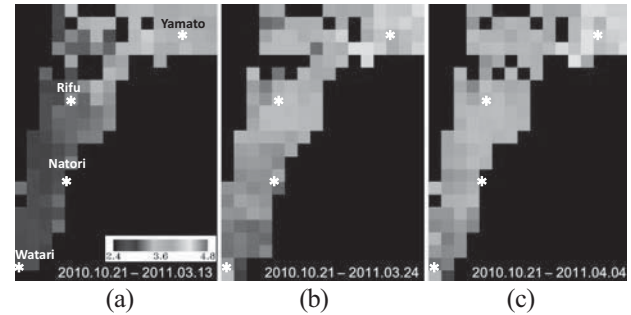


Figure 6 Detected displacement maps in the periods: Oct. 21, 2010 to March 13 (a), to March 24 (b) and to April 4, 2011 (c), shown in rainbow color.

5. VERIFICATION

To verify the accuracy and usefulness of the proposed method, we compared the detected results with the crustal movement data from GPS stations. Surface deformation is a vector in three-dimensional space with three components, D_E , D_N , and D_Z , in the east, north, and vertical directions, respectively. The relationship between an actual crustal movement and its shift in a SAR image is shown in Figure 7. SAR intensity images are geocoded with a spacing to the north and east directions, so the relationship between a crustal movement (D) and its shift (M) in a ground range SAR image can be described using Eq. (1).

$$\begin{pmatrix} M_E \\ M_N \end{pmatrix} = \begin{pmatrix} 1 & 0 & \cos \alpha / \tan \theta \\ 0 & 1 & \sin \alpha / \tan \theta \end{pmatrix} \begin{pmatrix} D_E \\ D_N \\ D_Z \end{pmatrix} \quad (1)$$

where D is the actual movement in the east, north, and vertical directions; M is the shift in the SAR image; α is the heading angle clockwise from north; and θ is the SAR incident angle.

The GPS recordings made at Yamoto, Rifu, Natori, and Watari stations from March 1 to April 25, 2011, were converted using Eq. (1) with a heading angle of 190.027° and a 37.313° incident angle, as shown in Figure 8. These three stations stopped immediately following the earthquake,

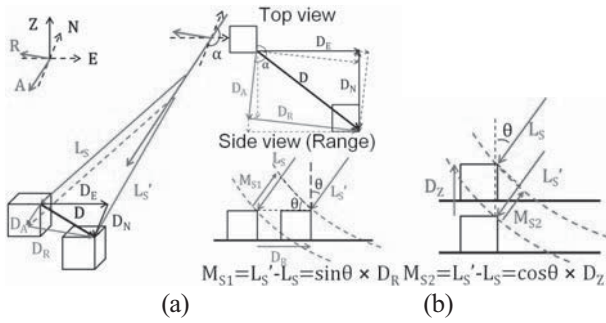


Figure 7 Schematic views of the horizontal (a) and vertical displacements (b) in a SAR image.

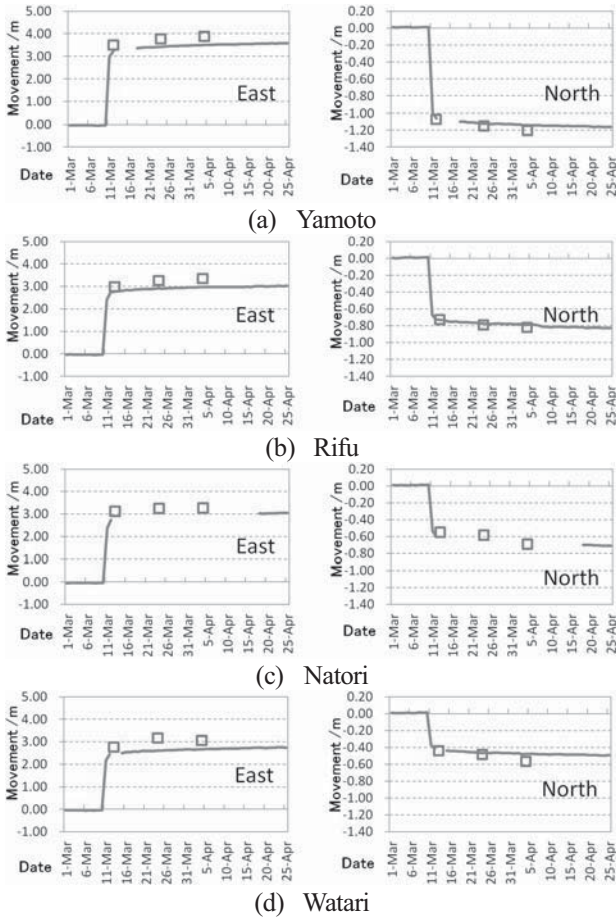


Figure 8 Comparison of movements converted from GPS data at Yamoto (a), Rifu (b), Natori (c), and Watari (d) ground control stations and the results detected in surrounding 13 km² sub-areas.

because they were affected by tsunamis. Natori station was the most seriously damaged and it did not restart until April 18, 2011. The measurement of ground movements in satellite images provides an important and effective tool in such cases. Since there were only the shifts of 3 buildings detected surrounding Natori station, the shift of the nearest building was used to compare with GPS data. A comparison of the results detected around a GPS station with the converted GPS recording demonstrated a very high level of consistency. Based on 11 comparison points, the averaged differences between the detected result and the GPS

measurement were about 0.38 m to the east and 0.02 m to the north. The maximum differences were less than 0.5 m to the east and 0.13 m to the north.

6. CONCLUSIONS

In this study, we proposed a method for detecting crustal movements due to a major earthquake on the basis of a comparison between two temporal SAR intensity images. The method was tested using four temporal TerraSAR-X images, including Sendai city before and after the 2011 Tohoku earthquake, and two temporal images of Tokyo. The four sub-areas surrounding GPS stations exhibited stable shifts of unchanged buildings, similar to the observed GPS data. Subpixel-based matching made it possible to detect movements with high accuracy, to within 0.5 m. However, the accuracy of our method depends on the location accuracy of the original images; hence, the accuracy may be lower when the method is applied to mountainous regions.

Acknowledgements:

The TerraSAR-X images used in this study were provided to the present authors by Pasco Corporation, Tokyo, Japan, as one of the funded projects of the SAR Data Application Research Committee.

References:

- Lee, J. S. (1980), "Digital image enhancement and noise filtering by use of local statistics," *Transactions on Pattern Analysis and Machine Intelligence*, IEEE, **PAMI-2** (2), 165–168.
- Massonnet, D., Rossi, M., Carmona, C., Adragna, F., Peltzer, G., Fiigl, K., and Rabaute, T. (1993), "The displacement field of the Landers earthquake mapped by radar interferometry," *Nature*, **364**, 138-142.
- Michel, R., Avouac, J.-P., and Taboury, J. (1999), "Measuring ground displacements from SAR amplitude image: application to the Landers earthquake," *Geophysical Research Letters*, IEEE, **26**(27), pp. 875-878.
- Stramondo, S., Cinti, F. R., Dragoni, M., Salvi, S., and Santini, S. (2002), "The August 17, 1999 Izmit, Turkey, earthquake: Slip distribution from dislocation modeling of DInSAR and surface offset," *Annals of Geophysics*, **45**(3/4), 527-536.
- Tobita, M., Suito, H., Imakiire, T., Kato, M., Fujiwara, S., and Murakami, M. (2006), "Outline of vertical displacement of the 2004 and 2005 Sumatra earthquakes revealed by satellite radar imagery," *Earth Planets Space*, **48**(1), e1-e4.
- Chini, M., Atzori, S., Trasatti, E., Bignami, C., Kyriakopoulos, C., Tolomei, C., and Stramondo, S. (2010), "The May 12, 2008, (Mw 7.9) Sichuan Earthquake (China): Multiframed ALOS-PALSAR DInSAR Analysis of Coseismic Deformation", *Geoscience and Remote Sensing Letters*, IEEE, **7**(2), 266-270.
- Eineder, M., Fritz, T., Mittermayer, J., Roth, A., Borner, E., Breit, H., and Brautigam, B. (2010), "TerraSAR-X Ground Segment Basic Product Specification Document," **1.7**, 31-32.